Condensed Matter Physics, 2004, Vol. 7, No. 4(40), pp. 683–698

CONDENSED MATTER PHYSICS

Car-Parrinello molecular dynamics simulations of Na^+–Cl^- ion pair in liquid water

J.M.Khalack [1,2] , A.P.Lyubartsev [2]

[1] Division of Physical Chemistry, Arrhenius Laboratory, Stockholm University, S–106 91 Stockholm, Sweden

[2] Bogolyubov Institute for Theoretical Physics of the National Academy of Sciences of Ukraine, 14b Metrologichna Str., 03143 Kyiv, Ukraine

Received August 16, 2004, in final form November 9, 2004

The aqueous solvation shell of a Na^+–Cl^- pair is studied using Car-Parrinello molecular dynamics simulations. Water-mediated and contact states of the ion pair are investigated. The first hydration shell of the Na^+ ion is found to be octahedral with one vacant position for both states. In the contact state one of the water molecules is substituted by the Cl^- ion. The first hydration shell of the Cl^- is less structured and strongly effected by the proximity of the Na^+ in the contact state. The oxygen coordination numbers for Na^+ and Cl^- are 4.9 and 5.6 for the water-mediated state, and 3.6 and 6.4 for the contact state. The corresponding hydrogen coordination numbers are 10.9 and 5.2; 9.2 and 3.9, respectively.

Key words: *ab initio molecular dynamics, hydration, Sodium ion, Chloride ion*

PACS: *61.20.Ja*

1. Introduction

Solvation of ions in aqueous solutions plays an important role in many chemical processes such as electrostriction and electrolyte dissociation. Aqueous solutions are also vital for biological systems. The intriguing selectivity of biological ionic channels has been related to the hydration structure of metal ions [1]. The hydration shell around an ion forms due to electrostatic interactions between the ion and the polarized water molecules. The presence of the solvation shell effects, in turn, the properties of the hydrated ions.

Experimental investigation of the structure of the solvation shells is extremely difficult because the relevant information is buried by the response of the bulk

water molecules [2–6]. Therefore the solvation structure around the ions is a major concern of theoretical investigations. Most of the theoretical studies have been done by means of molecular dynamics (MD) simulations employing empirical atom-atom interaction potentials [3,7–11]. The problem with the empirical interaction potentials lies in their variety as well as in the diversity of their parameters.

A recent review [12] provides a comparative study of six different force fields widely used in the simulation of systems containing aqueous Na^+ and Cl^- along with four different water models. The study demonstrates huge uncertainties in the height (more than one order of magnitude) and the position (up to 1 Å) of the first peak of the ion-ion radial distribution functions (RDF) obtained with the use of different interaction potentials.

The ion-oxygen RDFs calculated with different force fields are in much better agreement with each other, since there exist the experimental data inferred from the X-ray diffraction and the neutron scattering studies [2,4]. Experimental determination of the ion-ion RDFs would require unphysical ion concentrations in the solution. Therefore the most realistic way of refining the properties of the ion-ion distributions would involve the ab initio quantum mechanics calculations. Unfortunately, the fact that such calculations are computationally very demanding restricts the maximum size of a simulated system to the order of 10 Å. As a result, the main features of the equilibrium solvation structure of alkali metals have been investigated by considering the metal ions solvated in isolated water clusters [13,14]. The most extensive study of sodium chloride solvation [15] involves the NaCl molecule microsolvated with up to 10 water molecules, the NaCl being represented with restricted Hartree-Fock ab initio wave functions, and the water molecules being treated with the effective fragment potential model.

The additional information on the structural and the dynamic properties of the solvation complex can be obtained by the ab initio molecular dynamics simulations in the approach suggested by Car and Parrinello [16]. The approach combines the density functional theory (DFT) with molecular dynamics and permits to follow the dynamics of the system at the time scales of tens of picoseconds. It has been successfully applied to the investigation of many aqueous systems [17–19], including the solvation properties of single Na^+ [20] and Cl^- [21] ions.

In the present paper, we report the results of Car-Parrinello molecular dynamics (CPMD) simulations for an aqueous system containing both the Na^+ and the Cl^- ions. Special attention is paid to the properties of the hydration shell of the contact Na^+–Cl^- pair as compared to the hydration shells of single ions. The structural and dynamics properties are investigated.

2. Methods

The Car-Parrinello molecular dynamics approach treats the electronic subsystem in the approximation of the density functional theory, and the nuclei are considered

as classical particles. The approach is based on the Lagrangian [16]

$$\begin{aligned}\mathcal{L} &= \mu \sum_i \int \left|\dot{\phi}_i(\mathbf{r})\right|^2 \mathrm{d}\mathbf{r} + \frac{1}{2}\sum_I M_I \dot{\mathbf{R}}_I^2 - E\left[\{\phi_i\}, \{\mathbf{R}_I\}\right] \\ &\quad + \sum_{i,j} \Lambda_{ij}\left(\langle\phi_i|S\left(\{\hat{\mathbf{R}}_I\}\right)|\phi_i\rangle - \delta_{ij}\right), \end{aligned} \tag{1}$$

where the third term is the energy functional in the DFT formulation, the second term stands for the kinetic energy of the nuclei, and the first term is introduced to perform the dynamical simulated annealing of the electronic subsystem. The electron density $\rho(\mathbf{r})$ is written in terms of occupied single-particle electron orbitals (pseudowavefunctions) $\phi_i(\mathbf{r})$. These functions are subject to generalized orthonormality constraints maintained by means of the fourth term of equation (1), where Λ_{ij} are the Lagrange multipliers. The positions of nuclei are represented by $\mathbf{R}_I$. The parameters $\{\phi_i\}$ and $\{\mathbf{R}_I\}$ are dependent on time, and dots denote the time derivatives. Masses M_I are the physical masses of the nuclei, while the parameter μ is a fictitious mass introduced in order to anneal the electron density down to the Born-Oppenheimer surface with the course of time.

The energy functional $E\left[\{\phi_i\}, \{\mathbf{R}_I\}\right]$, also called Kohn-Sham [22] functional, is as follows:

$$\begin{aligned} E\left[\{\phi_i\}, \{\mathbf{R}_I\}\right] &= \frac{1}{2}\sum_i \left\langle \phi_i \left| -\nabla^2 \right| \phi_i \right\rangle + E_{xc}([\rho]) \\ &\quad + \frac{1}{2}\int\int \frac{\rho(\mathbf{r}_1)\rho(\mathbf{r}_2)}{|\mathbf{r}_1 - \mathbf{r}_2|}\mathrm{d}\mathbf{r}_1\mathrm{d}\mathbf{r}_2 + \frac{1}{2}\sum_{I\neq J}\frac{Z_I Z_J}{|\mathbf{R}_I - \mathbf{R}_J|} \\ &\quad + \int V_{\mathrm{L}}\left(\mathbf{r}, \{\mathbf{R}_I\}\right)\rho(\mathbf{r})\mathrm{d}\mathbf{r} + \sum_i \left\langle \phi_i \left| \hat{V}_{\mathrm{NL}}\left(\{\mathbf{R}_I\}\right) \right| \phi_i \right\rangle . \end{aligned} \tag{2}$$

The first term represents the physical kinetic energy of the electrons. $E_{\mathrm{xc}}([\rho])$ is the exchange–correlation part of the energy functional which stands to account for the exchange, correlation and other contributions to the total energy of electrons. The exact analytical expressions for this part is unknown. However, there exist several approximative expressions for it, such as local density approximation $E_{\mathrm{xc}}([\rho]) = \int \varepsilon_{\mathrm{xc}}(\rho(\mathbf{r}))\rho(\mathbf{r})\mathrm{d}\mathbf{r}$ [22]. The third and the fourth terms in equation (2) account for the Coulomb repulsion within electronic and nuclear subsystems, respectively. Interaction between the electrons and the nuclei (the last two terms) is usually described by pseudopotentials.

For the most common case of norm-conserving pseudopotentials, the electron density is written as $\rho(\mathbf{r}) = \sum_i |\phi_i(\mathbf{r})|^2$, and the overlap operator $\hat{S}$ in the orthonormality constraint is simply equal to 1. Since the norm-conserving pseudopotentials require a relatively high cutoff in the plane wave expansion of the electron malfunctions, the ultrasoft Vanderbilt pseudopotentials [23] have been devised. The approach permits to smoothen the wavefunctions $\phi_i(\mathbf{r})$ in the ionic core regions at a price that the electron density becomes augmented: $\rho(\mathbf{r}) = \sum_i \left[|\phi_i(\mathbf{r})|^2 + \sum_{nm,I} Q_{nm}^I(\mathbf{r})\langle\phi_i|\beta_n^I\rangle\langle\beta_m^I|\phi_i\rangle\right]$. The overlap operator in the generalized

orthonormality constraint of (1) becomes $\hat{S} = 1 - \sum_{nm,I} q_{nm} |\beta_n^I\rangle\langle\beta_m^I|$ with $q_{nm} = \int Q_{nm}(\mathbf{r})\mathrm{d}\mathbf{r}$ (the details concerning the augmentation functions can be found in [23]).

The equations of motion generated by the Lagrangian (1) are written as [24]:

$$\mu\ddot{\phi}_i = -\frac{\delta E[\{\phi_i\},\{\mathbf{R}_I\}]}{\delta\phi_i^*} + \sum_j \Lambda_{ij}\hat{S}\phi_j\,, \tag{3}$$

$$M_I\ddot{\mathbf{R}}_I = -\frac{\partial E[\{\phi_i\},\{\mathbf{R}_I\}]}{\partial\mathbf{R}_I} + \sum_{ij}\Lambda_{ij}\left\langle\phi_i\left|\frac{\partial\hat{S}}{\partial\mathbf{R}_I}\right|\phi_j\right\rangle. \tag{4}$$

Fictitious electronic temperature (defined by the mass μ and time derivatives of the electron wave functions ϕ_i) is kept low to hold electron wave functions in the vicinity of the energy minimum which corresponds to the Born-Oppenheimer approximation. More details on the Car-Parrinello approach can be found in the original papers [16,24] or in review [25].

3. Simulation details

The simulated system consisted of one Cl and one Na dissolved in 48 water molecules. The system was kept electroneutral, and the valence electrons were free to rearrange so as to give the charge distribution corresponding to the minimum of the Kohn-Sham energy functional. The electrons were considered to be spin paired so that they formed closed shells. The electron density distributions around the dissolved sodium and chloride ions were found to coincide with the electron density distributions around single Na^+ and Cl^- ions of the charge $+/-1$ correspondingly. The size of the cubic simulation cell with periodic boundary conditions was 11.382761 Å, providing the experimental density of salt solution at the corresponding concentration. The fictitious electron mass was 700 a.u., and the time step was 0.1 fs. Interactions of the nuclei with the valence electrons were represented by the Vanderbilt ultrasoft pseudopotentials [23,24], that allowed us to work with the Kohn-Sham orbitals $\phi_i(\mathbf{r})$ expanded in plane waves with a low energy cutoff of 25 Ry. The PBE [26] functional was employed to account for the exchange and correlation effects. The Car-Parrinello molecular dynamics simulations were performed using CPMD [27] code in the NVT ensemble. The Nosé–Hoover thermostat [28–30] was applied at 300 K.

To start the simulations, a short classical molecular dynamics run was performed to get an atomic configuration to be used as an input for DFT calculations. Then, the ground state single-particle electron orbitals $\{\phi_i(\mathbf{r})\}$ minimizing the energy functional (2) for the obtained atomic configuration were found. Then the Car-Parrinello molecular dynamics simulations were run. The first 3 ps of CPMD dynamics were considered as equilibration time and discarded. For the production runs, the computer facilities of PDC supercomputer center were engaged (16 CPUs of 900 MHz Intel Itanium Linux cluster [31]).

There were two production runs. In the first run the ions were initially located at the distance of ≈5 Å, corresponding to the position of the second maximum of Na^+–Cl^- radial distribution function in water reported for classical MD simulations [12].

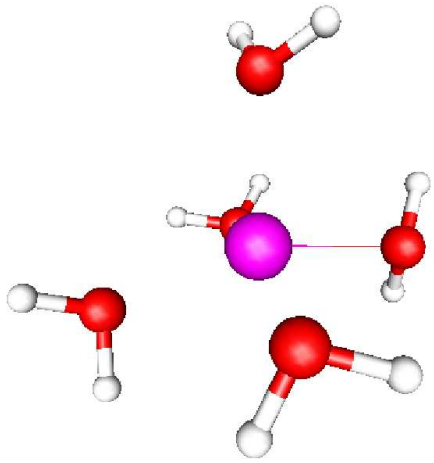

Figure 1. A typical snapshot of the first hydration shell of the Na^+ cation for the case of water-mediated ion pair. Oxygens of the water molecules are situated at the vertices of an octahedron, one of the six vertices being unoccupied.

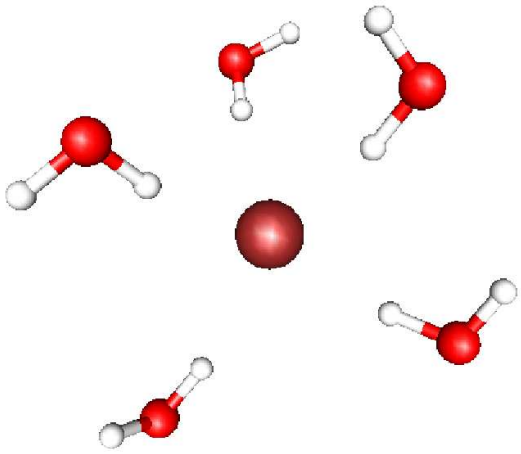

Figure 2. A typical snapshot of the first hydration shell of the Cl^- anion during the first simulation run.

The initial distance between the ions was chosen with the intention to observe possible transitions between water-mediated and contact states of the ion pair. Contrary to the expectations, the interionic distance was found to increase. The hydration shell of the Na^+ being practically invariable, the chloride anion underwent a gradual migration between the water molecules during ≈15 ps, until it was located at the third most probable distance from the cation. The process of migration seemed to be finalised by a change of one water molecule in the sodium hydration shell. Then the hydration shells of both atoms were found to resemble the hydration shells of single ions with fixed composition during the last 20 ps of simulations. The most probable number of water molecules in the first hydration shell was 5 for both ions.

Typical configurations of the first hydration shell around the Na^+ and the Cl^- ions during the second part of the first simulation run are shown in figures 1 and 2.

To gather the information on the hydration shell of a contact ion pair, the second simulation run was launched. In the second run the ions were initially put at a distance of 2.3 Å to get the closest possible arrangement of ions. Such an arrangement (see figure 3) was found to be stable during all 25 ps of the simulation, in agreement

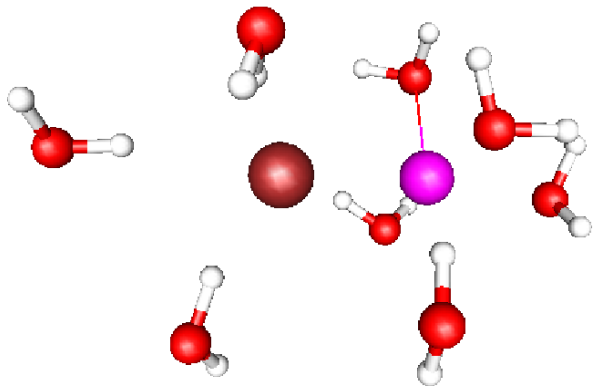

Figure 3. A typical snapshot of the hydration shell of the close Na^+–Cl^- pair. Oxygen of the water molecules around the sodium cation (on the right) are in a regular octahedral configuration, with one of the oxygens being substituted by the chloride anion. Another octahedral position (at the bottom) is left unoccupied. The water molecule seen on the right at the bottom of the panel is located at 3.4 Å distance from the Na^+ ion and belongs to the second hydration shell.

with the 30–100 ps range for the lifetime of the contact pair obtained from the classical MD simulations [12].

Accounting for the interionic distance in the two accomplished simulation runs, we will refer to the first simulated system as to the loose ionic pair. The second simulated system is referred to as the close pair, correspondingly.

4. Radial distribution functions

Radial distribution functions calculated independently for the two simulation runs are represented in figures 4–8. Unfortunately, we have not been able to reproduce the whole range of the Na–Cl distance distribution that is realised in physical sodium chloride solutions. The results from the first simulation run span the range from 3.8 Å to 8 Å, while the second simulation run covers the distances up to 3.2 Å. The absence of the observed transitions from water-mediated to contact state and vice versa, and the remaining gap between 3.2 Å and 3.8 Å do not make it possible to rely on the height of the first Na–Cl RD peak in figure 4. To fill in the gap, some additional computationally expensive constrained CPMD simulations [32] are to be done.

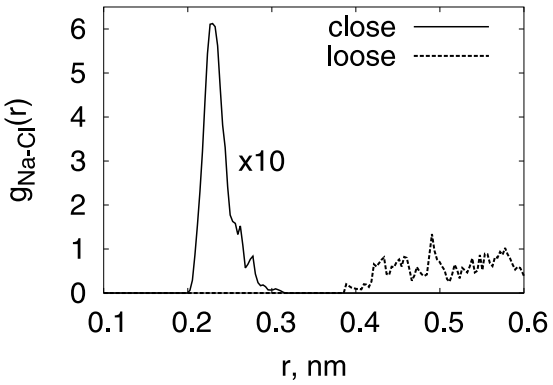

Figure 4. Na–Cl radial distribution functions for the two simulation runs. The interval from 3.2 Å to 3.8 Å is not covered by the simulations.

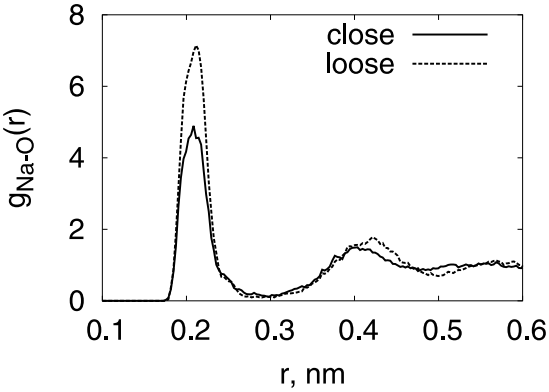

Figure 5. Na–O radial distribution functions for the two simulation runs.

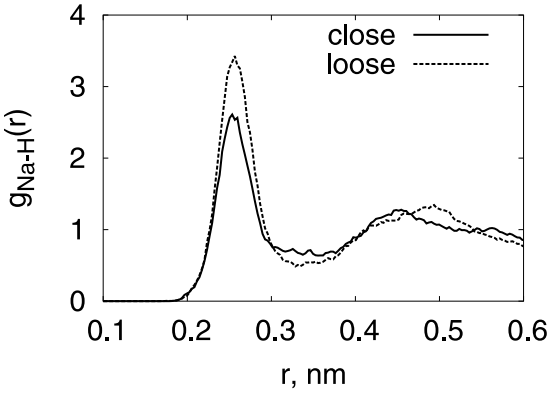

Figure 6. Na–H radial distribution functions for the two simulation runs.

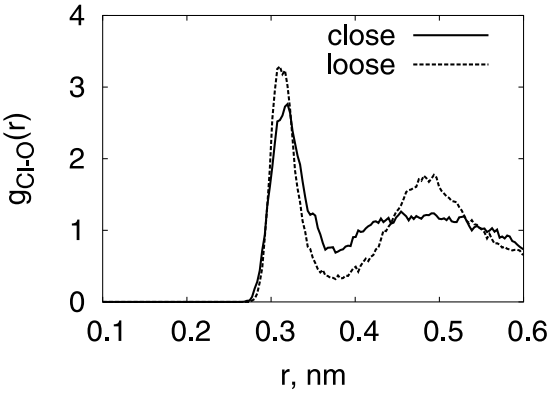

Figure 7. Cl–O radial distribution functions for the two simulation runs.

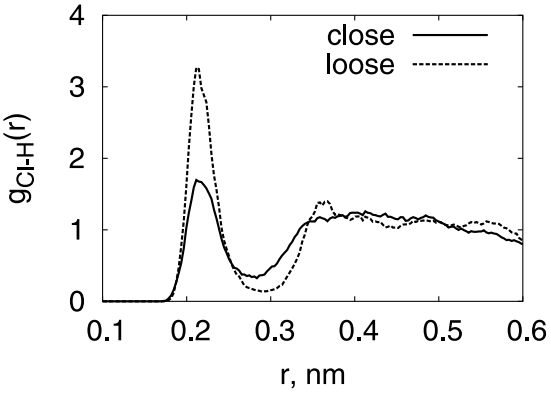

Figure 8. Cl–H radial distribution functions for the two simulation runs.

Noteworthy, the position of the first peak at 2.3 Å does not agree with the tendency of the Na–Cl distance to grow with the increase of the number of water molecules (amounting to 3.17 Å at n=10) observed in $NaCl(H_2O)_n$ ab initio cluster calculations [15]. Such a disagreement along with the difference of the hydration shell shown in figure 3 from the cluster configurations reported in [15] implies the importance of the second hydration shell in the solvation structure of aqueous sodium chloride.

Comparison of Na–O (figure 5) and Na–H (figure 6) RDFs for the case of water mediated (dashed line) and contact (solid line) ion pairs shows that the structure of the first hydration shell of the sodium cation remains practically unperturbed upon the substitution of one water molecule by the chloride anion (note the close resemblance in the positions of the first peaks of Na–O and Na–Cl RDFs). Indeed, such substitution changes the height, but not the position of the first Na–O and Na–H RDF peaks. The effect of the neighbouring Cl^- on the Na–O RDF begins at the second maximum, while the Na–H distribution is affected already at the first minimum.

The running oxygen coordination number $n_{\mathrm{NaO}}(r)$ of the Na^+ ion at the distance $r_{\mathrm{min}}^{\mathrm{NaO}}$=2.78 Å (the position of the first minimum of Na–O RDF) is 4.9 for the loose ion pair that compares favourably with 4.6±0.6 water molecules reported for the Na^+ dissolved in 32 waters [20]. For the contact pair $n_{\mathrm{NaO}}(r_{\mathrm{min}}^{\mathrm{NaO}})$=3.6. The change of the coordination number by 1.3 indicates that the presence of the negative Cl^- in the vicinity of the sodium cation actually diminishes the probability to find a water molecule at the vertex of the hydration octahedron. The hydrogen coordination number at the distance of the first Na–H RDF minimum ($r_{\mathrm{min}}^{\mathrm{NaH}}$=3.29 Å) amounts to 10.9 and 9.2 for the first and for the second simulation runs correspondingly.

For the contact pair, the high value of 9.2 includes even the hydrogens from the Cl^- hydration shell, since the protons hydrogen bonded to the anion (seen to the left from the Cl^- in figure 3) end up at a distance $\approx r_{\mathrm{min}}^{\mathrm{NaH}}$ from the sodium ion, changing the depth of the first minimum in figure 6.

The hydration shell of the chloride anion being less structured, it is more strongly effected by the neighbouring counterion. Figure 7 illustrates the displacement of the first peak of Cl–O RDF for the case of the contact pair. The first minimum at $r_{\mathrm{min}}^{\mathrm{ClO}}$=3.78 Å being less pronounced, the oxygen coordination number at $r_{\mathrm{min}}^{\mathrm{ClO}}$ becomes 6.4 as compared to the value of 5.6 for the water-mediated pair, and to 5.8 oxygen neighbour reported [21] for a single Cl^- dissolved in 64 water molecules. The increase in the number of oxygen neighbours is due to the water oxygens located in the first hydration shell of the Na^+ at the distance of ≈3.5 Å from the Cl^-. Apart from restructuring the first hydration shell, the close Na^+ neighbour smoothes out even the second hydration shell of the Cl^- as it is seen in figure 7. The presence of the contact ionic pairs in real solution could explain the relatively high experimental value of 6 [2] obtained for the Cl^- coordination number.

The Cl–H radial distribution functions (figure 8) reflect a substantial decrease in the number of hydrogen bonds accepted by the Cl^- anion with the appearance of a close Na^+ neighbour. Since the water molecules from the Na^+ hydration shell

do not donate hydrogen bonds to the Cl^-, the hydrogen coordination number falls down from 5.2 (5.2 for the single Cl^- ion [21]) to 3.9 at $r_{\min}^{\mathrm{ClH}}$=2.90 Å.

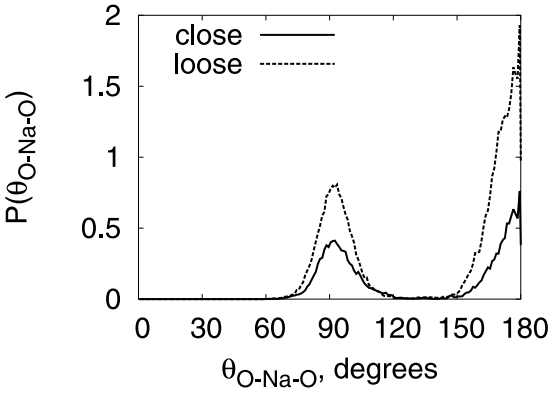

Figure 9. Distribution of O–Na–O angle in the Na^+ hydration shell. The maximum Na–O distance is 2.78 Å.

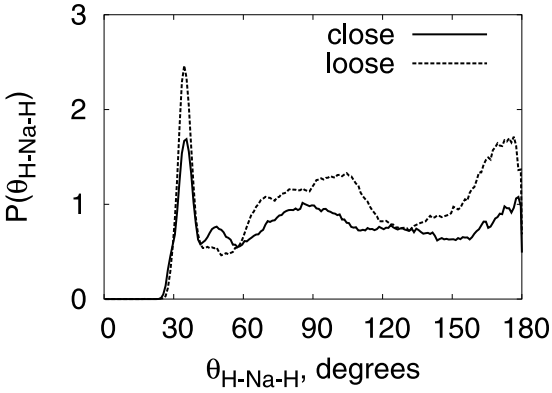

Figure 10. Distribution of H–Na–H angle in the Na^+ hydration shell. The maximum H distance from the sodium ion is 3.29 Å.

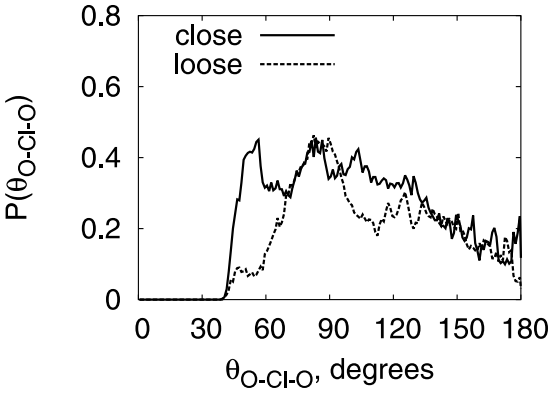

Figure 11. Distribution of O–Cl–O angle in the Cl^- hydration shell. The maximum Cl–O distance is 3.78 Å.

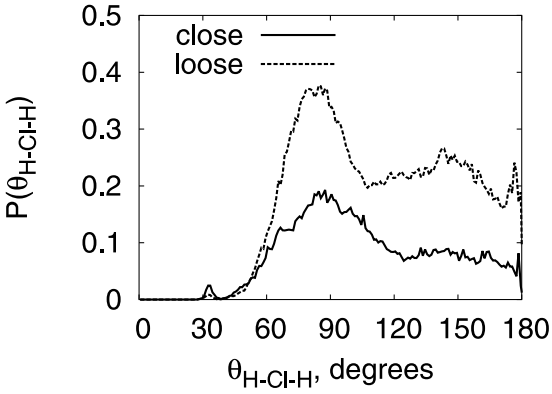

Figure 12. Distribution of H–Cl–H angle in the Cl^- hydration shell. The maximum H distance from the chloride ion is 2.9 Å.

5. Angle distributions

The radial distribution functions providing the information comparable to the experimental data, the structure of the hydration shell of an ion can be made more clear by plotting the distributions of the angles between the directions to the atoms constituting the hydration shell. To illustrate the change in coordination numbers, in figures 9–14 we plot the angle distribution functions $P(\theta)$ normalized so as to

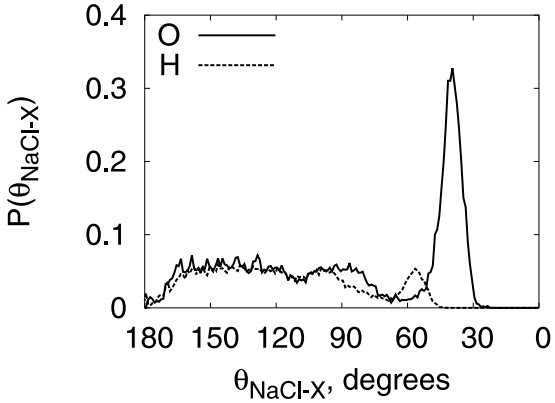

Figure 13. Distribution of Na–Cl–H (dashed line) and Na–Cl–O (solid line) angles in the hydration shell of the Cl^- ion from the close ion pair. The maximum distance from the chloride anion is 2.9 Å for hydrogens and 3.77 Å for oxygens. Note the inverse direction of the θ_{NaClX} axis.

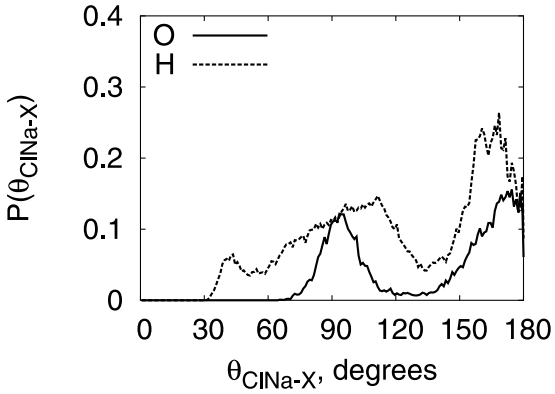

Figure 14. Distribution of Cl–Na–H (dashed line) and Cl–Na–O (solid line) angles in the hydration shell of the Na^+ ion from the close ion pair. The maximum distance from the sodium ion is 3.29 Å for hydrogens and 2.78 Å for oxygens.

integrate to the number N of the atoms found within the sphere of radius $r_{\max}$:

$$2\pi \int_0^{\pi} P(\theta) \sin\theta \mathrm{d}\theta = N. \tag{5}$$

The maximum radius $r_{\max}$ is chosen to equal the position of the first minimum of the corresponding RDF.

Figure 9 supports the octahedral structure of the sodium hydration shell by confirming 90° and 180° values of O–Na–O angles for both water-mediated and contact ion pairs.

The hydrogen atoms being the outer ones in the hydration shell of the cation, the distributions of H–Na–H angles (figure 10) are much smoother than the oxygen angle distributions. Still there exist broad maxima around 90° and 180°, and the distribution calculated for the contact pair is much less structured. The peak at

$\approx 35°$ is due to the hydrogen atoms belonging to the same water molecule.

Distributions of O–Cl–O (figure 11) and H–Cl–H (figure 12) angles in the hydration shell of the Cl^- anion from the water-mediated ion pair practically follow each other, in accordance with the hydrogen bonding existing between the water molecule and the Cl^- anion. Both distributions have a strong maximum between 60° and 105° centred at 80° along with a much less pronounced maximum centred at $\approx 130°$ for oxygens and at $\approx 140°$ for hydrogens. Almost the same angle distributions have been reported for the single Cl^- anion [21]. The authors of [21] have suggested the surrounding geometry to be close to octahedral. We would prefer to describe this geometry as being octahedral only for three water molecules (the top molecules in figure 2), the other two being opposed to the first three with the resulting $120° - 150°$ O–Cl–O angles.

The introduction of the sodium counterion into the first hydration shell of the Cl^- ion leads to a decrease in the number of accepted hydrogen bonds, broadening of the octahedral H–Cl–H maximum to 120°, as well as to unproportional decrease of the possibility to observe large H–Cl–H angles (see figure 12). The effect of the neighbouring Na^+ on the O–Cl–O distribution (figure 11) is even more drastic, since the octahedral maximum is almost washed out by the appearance in the Cl^- hydration shell of the water molecules declined by 90°–120° from the hydrogen bonded ones. Such molecules belong to the Na^+ hydration shell and form the additional maximum of O–Cl–O distribution at 50°.

Additional information on the hydration structure of the contact Na^+–Cl^- pair can be referred to from monitoring the declination of water molecules from the ion-ion axis. Figure 13 shows distributions of Na–Cl–H and Na–Cl–O angles for water molecules belonging to the Cl^- hydration shell. Due to the reversion of the horizontal axis, the hydrogen bonded water molecules found on the left in figure 3 contribute to (very smooth) left-side part of the angle distributions in figure 13. Correspondingly, the highly structured water molecules from the Na^+ hydration shell found on the right in figure 3 form the strong Na–Cl–O maximum at 40° and the Na–Cl–H maximum at 60° in the right-hand part of figure 13. The rightmost water molecule in figure 3 does not contribute to the angle distributions in figure 13 due to its large distance from the chloride ion.

The distribution of Cl–Na–O angles for water molecules from the first Na^+ hydration shell (figure 14) confirms the substitution of a water molecule by the Cl^- ion in the octahedrally structured sodium hydration shell (cf. figure 9). The distribution of Cl–Na–H angles in figure 14 follows the oxygen distribution, and the weak peak at 40° comes from the water molecules hydrogen bonded to the Cl^- anion.

The highly structured Na^+ hydration shell as compared to the less structured Cl^- hydration shell is clearly manifested in the spatial distributions of oxygen and hydrogen atoms around the contact ion pair. Figure 15 represents isosurfaces of spatial distribution functions (SDF) calculated in the reference frame formed by Na^+, Cl^-, and one of the closest water oxygens. Despite the fact that the centre of the distributions is located at the Cl^- ion, all notable maxima are found in the vicinity of the Na^+. Since even the water maximum opposite to the Cl^- ion (at the

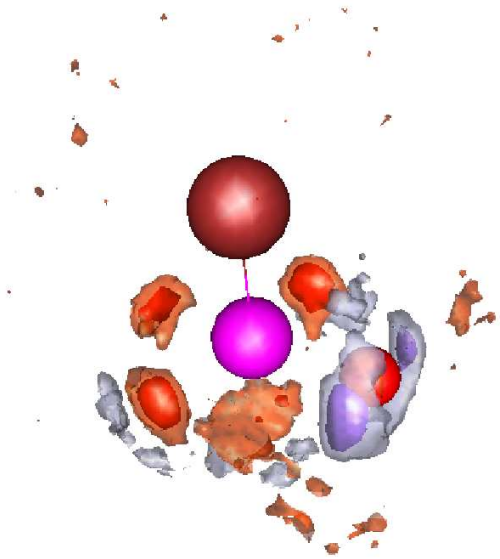

Figure 15. Isosurfaces of spatial distribution functions for O and H in the hydration shell of the close pair. SDF levels for oxygens are 25 and 10, and for the hydrogen atoms the levels are 20 and 8.

bottom of figure 15) is reproduced, the chosen SDF levels seem to be sufficiently low to be capable of reproducing the Cl^- hydration shell maxima if they did exist.

6. Dynamic properties

Structural properties of the Na^+ and Cl^- hydration shells correlate with the shell exchange dynamics. Lifetimes of water molecules in the more structured Na^+ hydration shell are significantly longer than corresponding lifetimes for the less structured Cl^- hydration shell. During the whole simulation time two water molecule exchange acts in the Na^+ hydration shell for the water-mediated ion pair and one exchange act for the Na^+ in the contact ion pair took place. The observed exchange acts differ from those considered in [8] by means of classical MD simulations. Since the sodium coordination number is less than 6, the incoming water molecule takes an unoccupied octahedron vertex, and the leaving water molecule starts off from another octahedron vertex. The moments of coming and leaving do not coincide in time.

The less structured Cl^- hydration shell is characterized by more intensive exchange dynamics. While the lifetime of water molecules in the hydration shell of the Cl^- ion from the contact pair agrees well with the 12 ps value reported for the single Cl^- [21], the waters are found to spend 3 to 8 ps in the hydration shell of the migrating Cl^- in the water-mediated Na^+–Cl^- pair.

The short-scale dynamics of the atomic species can be characterized by the power spectra of their velocity autocorrelation functions. To reduce the uncertainties due to the modest sampling for the correlation functions and to smooth out the Fourier spectra, we analyse the velocity autocorrelation functions by segments of the width $T = 1024$ fs. Segments are overlapped by one half of their length. The Welch window

[33]

$$W(t) = 1 - (2t/T - 1)^2 \tag{6}$$

is used to prevent the leakage from one frequency to another.

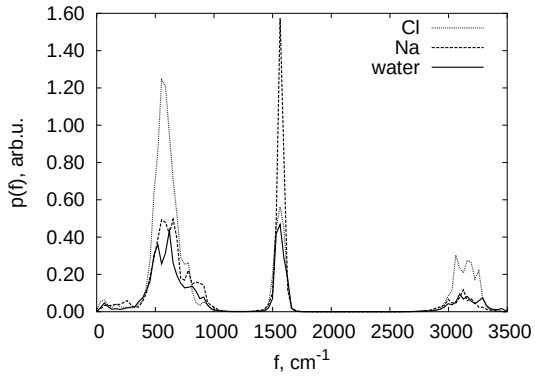

Figure 16. Velocity autocorrelation power spectra for hydrogen atoms from the Na^+ hydration shell (dashed line), the Cl^- hydration shell (dotted line), and bulk water molecules (solid line) for the system with the water-mediated ion pair.

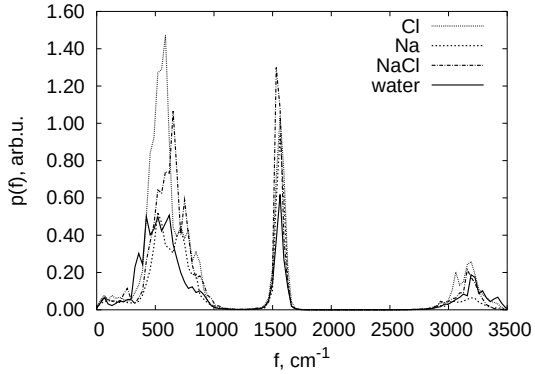

Figure 17. Velocity autocorrelation power spectra for hydrogen atoms belonging to the Na^+ hydration shell (dashed line), the Cl^- hydration shell (dotted line), both hydration shells (dash-dotted line), and to bulk water molecules (solid line) for the system with the contact ion pair.

The resulting velocity autocorrelation power spectra calculated separately for the hydrogen atoms from the water molecules belonging to the Na^+ hydration shell, the Cl^- hydration shell, and to bulk water are shown in figures 16–17. For the case of water-mediated ion pair (figure 16), the three spectra reproduce each other quite well, the only difference being in the intensities of the peaks. While the hydrogen bonding to the Cl^- anion prevents the development of the bending vibrations at 1600 cm^{-1}, the geometry of the Na^+ hydration shell on the contrary favours such vibrations. For the case of the contact pair (figure 17), the proximity of both ions

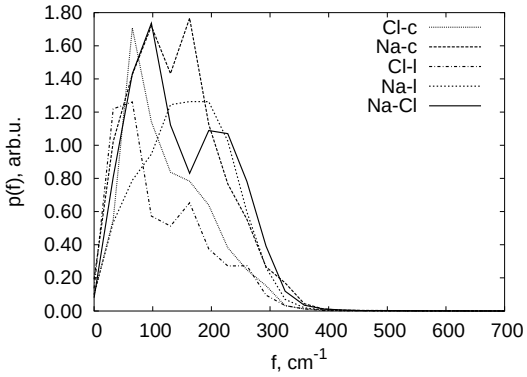

Figure 18. Velocity autocorrelation power spectra for oxygens from the Na^+ hydration shell (long-dashed line for the close pair and short-dashed line for the loose pair), for oxygens from the Cl^- hydration shell (dotted line for the close pair and dash-dotted line for the loose pair), and for the contact Na–Cl pair (solid line).

evens out the intensities of the peaks. Worth noting is a shoulder of the libration peak at ≈800 cm^{-1} seen for the hydrogens from the Na^+ hydration shell.

The velocity autocorrelation power spectra for the heavy atoms are presented in figure 18. While the frequencies of oxygen oscillations in the Cl^- hydration shell increase slightly upon the formation of the contact ion pair, the spectra of oxygen oscillations in the Na^+ hydration shell acquire a new frequency at ≈100 cm^{-1} (see long-dashed line as compared to short-dashed line). The same frequency appears in the spectrum of the relative Na–Cl motions (solid line), probably implying the concerted oscillating motion of the hydrated Na^+ with a period of ≈300 fs.

7. Conclusions

The Car-Parrinello molecular dynamics simulations of the Na^+–Cl^- ion pair dissolved in water demonstrate the existence of strongly structured octahedral hydration shell around the Na^+ ion with the most probable coordination number being 5. For the case of a Cl^- ion being in contact with Na^+, the anion substitutes one of the hydration molecules, and the octahedral structure remains unchanged. The hydration shell of the Cl^- is less structured and more strongly affected by the contact with the cation.

The obtained radial distribution functions can be used in constructing [18,34,35] a classical Na^+–Cl^- force field, provided the remaining gap in the Na–Cl distribution is filled in. The Car-Parrinello simulations performing the umbrella sampling of the gap are currently in progress, and the results will be reported elsewhere.

The present simulations have not taken into account the nuclear quantum effects on the dynamics of hydrogen atoms. These effects have been shown to be significant in forming the structure of liquid water [36] and are expected to effect the structure of

the ionic hydration shells. Fast developments in the computer performance promise that these effects will be widely simulated in the nearest future.

Acknowledgements

We thank the Center for Parallel Computers (PDC) at the Royal Institute of Technology in Stockholm for granting computer facilities. The work was supported by the Swedish Research Council (Vetenskapsrådet).

References

1. Degreve L., Vechi S.M., Quintale C. // Biochimica et Biophysica Acta – Bioenergetics, 1996, vol. 1274, No. 3, p. 149–156.
2. Bergström P.A., Lindgren J., Kristiansson O. // J. Phys. Chem., 1991, vol. 95, No. 22, p. 8575–8580.
3. Steel E.A., Merz J.K.M., Selinger A., Castleman J.A.W. // J. Phys. Chem., 1995, vol. 99, No. 19, p. 7829–7836.
4. Neilson G.W., Enderby J.E. // J. Phys. Chem., 1996, No. 4, vol. 100, p. 1317–1322.
5. Fischer W.B., Fedorowicz A., Koll A. // Phys. Chem. Chem. Phys., 2001, vol. 3, No. 19, p. 4228–4234.
6. Patwari G.N., Lisy J.M. // J. Chem. Phys., 2003, vol. 118, No. 19, p. 8555–8558.
7. Dang L.X., Smith D.E. // J. Chem. Phys., 1993, vol. 99, No. 9, p. 6950–6956.
8. Rey R., Hynes J. T. // J. Phys.: Condens. Matter, 1996, vol. 3, No. 47, p. 9411–9416.
9. Carrillo-Tripp M., Saint-Martin H., Ortega-Blake I. // J. Chem. Phys., 2003, vol. 118, No. 15, p. 7062–7073.
10. Perera L., Berkowitz M. // J. Chem. Phys., 1994, vol. 100, No. 4, p. 3085–3093.
11. Lukyanov S.I., Zidi Z.S., Shevkunov S.V. // J. of Molecular Structure, 2003, vol. 623, p. 221–236.
12. Patra M., Karttunen M. // J. Comput. Chem., 2004, vol. 25, No. 5, p. 678–689.
13. Glendening E.D., Feller D. // J. Phys. Chem., 1995, vol. 99, No. 10, p. 3060–3067.
14. Hashimoto K., Kamimoto T., Fuke K. // Chem. Phys. Lett., 1997, vol. 266, No. 1–2, p. 7–15.
15. Petersen C.P., Gordon M.S. // J. Phys. Chem. A, 1999, vol. 103, No. 21, p. 4162–4166.
16. Car R., Parrinello M. // Phys. Rev. Lett., 1985, vol. 55, p. 2471–2474.
17. Ramaniah L., Bernasconi M., Parrinello M. // J. Chem. Phys., 1999, vol. 111, No. 4, p. 1587–1591.
18. Lyubartsev A.P., Laasonen K., Laaksonen A. // J. Chem. Phys., 2001, vol. 114, No. 7, p. 3120–3126.
19. Boek E.S., Sprik M. // J. Phys. Chem. B, 2003, vol. 107, No. 14, p. 3251–3256.
20. Rempe S.B., Pratt L.R. // Fluid Phase Equilibria, 2001, vol. 183-184, p. 121–132.
21. Heuft J.M., Meijer E.J. // J. Chem. Phys., 2003, vol. 119, No. 22, p. 11788–11791.
22. Kohn W., Sham L.J. // Phys. Rev., 1965, vol. 140, No. 4A, p. 1133–1138.
23. Vanderbilt D. // Phys. Rev. B, 1990, vol. 41, No. 11, p. 7892–7895.
24. Laasonen K., Pasquarello A., Car R., Lee C., Vanderbilt D. // Phys. Rev. B, 1993, vol. 47, No. 16, p. 10142–10153.

25. Galli G., Parrinello M. Ab initio molecular dynamics: principles and practical implementation. – In: Computer Simulation in Material Science. Edited by Meyer M., Pontikis V., Kluwer Academic Publishers, 1991, p. 283–304.
26. Perdew J.P., Burke K., Emzerhof M. // Phys. Rev. Lett., 1996, vol. 77, No. 18, p. 3865–3868.
27. J. Hutter *et al.* CPMD version 3.7.2. Copyright IBM Corp 1990–2004. Copyright MPI für Festkörperforschung Stuttgart 1997–2001.
28. Nosé S. // Mol. Phys., 1984, vol. 52, No. 2, p. 255–268.
29. Hoover W. // Phys. Rev. A, 1985, vol. 31, p. 1695–1697.
30. Martyna, G.J., Klein, M.L., Tuckerman, M. // J. Chem. Phys., 1992, vol. 97, No. 4, p. 2635–2643.
31. *Lucidor* Intel Itanium 900 MHz Linux cluster. Center for Parallel Computers, KTH – Royal Institute of Technology, Stockholm, Sweden. http://www.pdc.kth.se.
32. Sprik M., Ciccotti G. // J. Chem. Phys., 1998, vol. 109, p. 7737.
33. Press W.H., Teukolsky S.A., Vetterling W.T. Numerical Recipes in C, 2nd ed. Cambridge University Press, 1993.
34. Lyubartsev A., Laaksonen A. // Phys. Rev. E, 1995, vol. 52, No. 4, p. 3730–3737.
35. Lyubartsev A., Marcelja S. // Phys. Rev. E, 2002, vol. 65, No. 4, p. 041202.
36. Chen B., Ivanov I., Klein M., Parrinello M. // Phys. Rev. Lett., 2003, vol. 91, No. 21, p. 215503.

Моделювання іонної пари Na^+–Cl^- у рідкій воді за методом молекулярної динаміки Кара-Паррінелло

Ю.М.Халак [1,2], А.П.Любарцев [2]

[1] Відділ фізичної хімії, Стокгольмський університет, лабораторія ім. Арреніуса, 106 91 Стокгольм, Швеція

[2] Інститут теоретичної фізики ім. М.М. Боголюбова, Національна Академія наук України, вул. Метрологічна 14–б, Київ–143, 03143 Україна

Отримано 16 серпня 2004 р., в остаточному вигляді – 9 листопада 2004 р.

Методами молекулярної динаміки Кара-Паррінелло вивчалася гідратна оболонка іонної пари Na^+–Cl^-. Досліджувалися медійований водою та контактний стан іонної пари. Знайдено, що перша гідратна оболонка іону Na^+ є виражено октаедричною в обох станах. У контактному стані має місце заміщення однієї з молекул води іоном хлору. Перша гідратна оболонка іону Cl^- є менш структурованою й на неї сильніше впливає близькість іону натрію у контактній парі. Кисневі координаційні числа іонів натрію і хлору дорівнюють 4.9 та 5.6 для медійованого водою стану, та 3.6 і 6.4 для контактного стану іонної пари. Відповідні водневі координаційні числа становлять 10.9 і 5.2 та 9.2 і 3.9.

Ключові слова: *молекулярна динаміка з перших принципів, гідратація, іон натрію, іон хлору*

PACS: *61.20.Ja*